Towards Stable Second-Kind Boundary Integral Equations for Transient Wave Problems

D. Hoonhout¹, C. Urzúa-Torres^{1*}

¹Delft Institute of Applied Mathematics, TU Delft, Mekelweg 4, 2628CD Delft, The Netherlands

Abstract

In this paper, we discuss the stable discretisation of the double layer boundary integral operator for the wave equation in 1d. For this, we show that the boundary integral formulation is L^2 -elliptic and also inf-sup stable in standard energy spaces. This turns out to be a particular case of a recent result on the inf-sup stability of boundary integral operators for the wave equation and contributes to its further understanding. Moreover, we present the first BEM discretisations of second-kind operators for the wave equation for which stability is guaranteed and a complete numerical analysis is offered. We validate our theoretical findings with numerical experiments.

1 Introduction

Time-domain boundary integral equations (BIEs) and boundary element methods (BEM) for the transient wave equation are well-established in the literature. We refer to [1, 2, 3, 12, 16, 23, 26, 30, 32, 33] and the references therein, to mention a few. However, in spite of their broad use and success, its numerical analysis is still incomplete, as pointed out in [12, 26].

Most of the current literature is based on the groundbreaking work of Bamberger and Ha-Duong [3], where they proposed a time-dependent variational formulation for transient wave problems for which existence and uniqueness is shown using the Laplace transform. Their results established ellipticity and continuity in different weighted Sobolev spaces. This so-called *norm gap* prevents the use of standard numerical analysis tools such as the Lax-Milgram theorem.

Later, Aimi et al. introduced a different formulation [2], usually referred to as $Energetic\ BEM$, which is elliptic and continuous in L^2 for one dimensional problems, thus providing a complete error and stability analysis in 1d. Numerical evidence also supports their applicability in 2d. Nonetheless, to the best

^{*}The research leading to this publication received funding from the Dutch Research Council (NWO) under the NWO-Talent Programme Veni with the project number VI.Veni.212.253.

of the authors' knowledge, no numerical analysis of this method is available for higher dimensions. In addition, energetic BEM for Neumann problems requires higher regularity on the ansatz space than the expected one (which is a drawback for overly perfectionist mathematicians).

More recently, Steinbach and Urzúa-Torres developed a new space-time formulation [36] that does not suffer from a norm-gap and for which existence and uniqueness is proven with the expected regularity in all dimensions. In order to achieve this, they had to work in a more general framework. Instead of ellipticity, they showed inf-sup stability of the BIEs in a new family of trace spaces, which preserve the expected regularity in space and time. Furthermore, in joint work with Zank [37], they regularised their formulation by means of the *Modified Hilbert transform*. The resulting variational form is proven to be elliptic in the natural energy spaces and can also be seen as a generalisation of the energetic BEM approach. This last result is currently only available in 1d.

There is still a lot to comprehend about the new framework introduced by Steinbach and Urzúa-Torres. In this paper, we aim to understand this further and work with the second-kind formulation from [36]. Moreover, as a first step in this direction, we consider only one spatial variable and propose two stable space-time Galerkin discretisations for the second-kind BIE that corresponds to the transient wave equation with prescribed Dirichlet data in 1d. For this, we develop the analysis both in L^2 , and in the natural trace space $H_{0,}^{1/2}(\Sigma)$ and its dual space $[H_{0,}^{1/2}(\Sigma)]'$. Moreover, we show that the corresponding second-kind formulations have a unique solution when considering these spaces. Finally, we prove that the proposed discretisation is stable under certain mesh conditions, that agree with the ones found in [24].

The introduced approach distinguishes itself from existing methods in 1d in a variety of ways: (i) The regularity assumption on the Dirichlet data is weakened, when compared with energetic BEM; (ii) It does *not* require stabilisation by introducing operators such as the Modified Hilbert transform, and thus has a simpler implementation than [37]; (iii) Numerical results show that it works for all meshes where the L^2 -orthogonal projection is H^1 -stable, and thus retains the potential use of space-time adaptive algorithms and parallelisation.

The novelty and appeal of this approach relies on its simplicity and on the fact that it offers the first standalone stable second-kind formulation for the wave equation, which benefits from the well-conditioning of this type of BIEs. Although this paper focuses on 1d and the analysis we provide cannot be extended directly, the message we hope to convey is that there is no reason to believe that second kind formulations for the wave equation are hopeless. Moreover, they may actually offer some computational advantages.

Indeed, the literature regarding BEM for transient wave problems mainly focuses on *first-kind* formulations and its discretisation. The review article by Costabel and Sayas [12] gives an extensive overview of the currently available approaches. Examples of these works include [16, 17, 18, 19, 30, 32]. Some of the few cases that examine *second-kind* formulations are [22], and [14, 5] where combined field approaches are required for stability.

This paper is structured as follows: In Section 2, we briefly introduce the required mathematical framework. Then we show in Section 3 that the bilinear forms for the second-kind variational formulation proposed in [36] are isomorphisms both in the natural energy space and even elliptic in L^2 when restricted to one spatial-dimension. Section 4 is dedicated to present the two related discretisations, namely, using piecewise constant basis functions as test and trial spaces, and using piecewise linear basis functions with zero initial condition. We complete the Section by showing discrete inf-sup stability for the latter. In Section 5, we proceed to derive the corresponding error estimates. Finally, we provide numerical experiments in Section 6 to validate our theoretical claims.

2 Preliminaries

2.1 Model problem

Let Ω be an interval $\Omega=(0,L)\subset\mathbb{R}$, with boundary $\Gamma=\{0,L\}$. For a finite time interval (0,T), we define the interior space-time cylinder $Q:=\Omega\times(0,T)\subset\mathbb{R}^2$, and its lateral boundary $\Sigma:=\Gamma\times[0,T]$. In an analogous fashion, the exterior space-time cylinder is denoted by $Q_{ext}:=(\mathbb{R}\setminus\overline{\Omega})\times(0,T)$.

We denote the D'Alembert operator by $\Box := \partial_{tt} - \Delta_x$, and write the interior Dirichlet initial boundary value problem for the wave equation as

$$\begin{array}{rcl} \square u(x,t) & = & f(x,t) & \quad \text{for } (x,t) \in Q, \\ u(x,t) & = & g(x,t) & \quad \text{for } (x,t) \in \Sigma, \\ u(x,0) = \partial_t u(x,t)_{|t=0} & = & 0 & \quad \text{for } x \in \Omega, \end{array} \tag{1}$$

and the exterior Dirichlet initial boundary value problem for the wave equation

$$\Box u(x,t) = f(x,t) \quad \text{for } (x,t) \in Q_{ext},
 u(x,t) = g(x,t) \quad \text{for } (x,t) \in \Sigma,
 u(x,0) = \partial_t u(x,t)_{|t=0} = 0 \quad \text{for } x \in \Omega.$$
(2)

The fundamental solution of the wave equation in 1d is $G(x,t) = \frac{1}{2} H(t-|x|)$, with H the Heaviside step function.¹

Let \mathcal{D} denote the double layer potential, defined as usual as

$$(\mathscr{D}z)(x,t) := \int_0^t \int_{\Gamma} \partial_{n_y} G(x-y,t-\tau) \, z(y,\tau) \, ds_y \, d\tau, \tag{3}$$

for $(x,t) \in Q$ and a regular enough density z.

We can represent the solution u of (1) by using the double layer potential [33, Ch. 1]. Hence, we solve the following boundary integral equation (BIE) of the second-kind

$$\left(-\frac{1}{2}\operatorname{Id} + \mathsf{K}\right)z = g,\tag{4}$$

¹While
$$G(x,t) = \frac{1}{2\pi} \frac{\mathsf{H}(t-|x|)}{\sqrt{t^2-|x|^2}}$$
 in $2d$, and $G(x,t) = \frac{1}{4\pi} \frac{\delta(t-|x|)}{|x|}$ in $3d$.

where Id is the identity and K the *double layer operator*, which will be defined in Section 2.3. Similarly, we solve [11, Sec. 4]

$$\left(\frac{1}{2}\operatorname{Id} + \mathsf{K}\right)z = g,\tag{5}$$

when considering the exterior problem (2). We dedicate the next section to introduce the mathematical framework required to properly state these BIEs.

2.2 Mathematical framework for 1d

Let $\mathcal{O} \subseteq \mathbb{R}^m$, m=1,2. We stick to the usual notation for the space $L^2(\mathcal{O})$ of Lebesgue square integrable functions; and the Sobolev spaces $H^s(\mathcal{O})$. Moreover, inner products of Hilbert spaces X are denoted by standard brackets $(\cdot, \cdot)_X$, while angular brackets $\langle \cdot, \cdot \rangle_{\mathcal{O}}$ are used for the duality pairing induced by the extension of the inner product $(\cdot, \cdot)_{L^2(\mathcal{O})}$. For a Hilbert space X we denote by X' its dual with duality pairing $\langle \cdot, \cdot \rangle_{\mathcal{O}}$.

We consider the spaces

$$\begin{split} H^1_{0,}(0,T;L^2(\Omega)) &:= & \Big\{ v \in L^2(Q) : \partial_t v \in L^2(Q), \ v(x,0) = 0 \quad \text{for } x \in \Omega \Big\}, \\ H^1_{,0}(0,T;L^2(\Omega)) &:= & \Big\{ v \in L^2(Q) : \partial_t v \in L^2(Q), \ v(x,T) = 0 \quad \text{for } x \in \Omega \Big\}. \end{split}$$

With these, we introduce

$$H^1_{:0.}(Q) := L^2(0,T;H^1(\Omega)) \cap H^1_{0.}(0,T;L^2(\Omega)),$$

which has zero initial values at t = 0; and

$$H^1_{:,0}(Q) \ := \ L^2(0,T;H^1(\Omega)) \cap H^1_{,0}(0,T;L^2(\Omega)),$$

which prescribes zero final values at t = T. We remark that these are Hilbert spaces with norms $||u||_{H^1_{;0,}(Q)} := |u|_{H^1(Q)}$ and $||v||_{H^1_{;,0}(Q)} := |u|_{H^1(Q)}$, where $|u|_{H^1(Q)} := \sqrt{||\partial_t u||^2_{L^2(Q)} + ||\nabla_x u||^2_{L^2(Q)}}$.

We note that the space $L^2(\Sigma)$ boils down to $L^2(\Sigma) = L^2(0,T) \times L^2(0,T)$ in 1d. Furthermore, we consider the spaces

$$H_{0,}^{1}(\Sigma) := \{ v = \begin{pmatrix} v_{0} \\ v_{L} \end{pmatrix} : v_{0}, v_{L} \in H^{1}(0, T), v_{0}(0) = v_{L}(0) = 0 \}, \tag{6}$$

and

$$H_{0}^{1}(\Sigma) := \{ v = \begin{pmatrix} v_{0} \\ v_{L} \end{pmatrix} : v_{0}, v_{L} \in H^{1}(0, T), v_{0}(T) = v_{L}(T) = 0 \}.$$
 (7)

Finally, we define $H_{0,}^{1/2}(\Sigma)$, and $H_{0,0}^{1/2}(\Sigma)$ by interpolation as [31, Sect. 2.1.7]

$$H_{0,}^{1/2}(\Sigma):=[H_{0,}^{1}(\Sigma),L^{2}(\Sigma)]_{\theta=1/2}, \qquad H_{,0}^{1/2}(\Sigma):=[H_{,0}^{1}(\Sigma),L^{2}(\Sigma)]_{\theta=1/2}.$$

Then we have the following result:

Lemma 2.1 ([36, Lemmas 3.1 and 3.2]). The mappings

$$\gamma_{\Sigma}^{i}: H_{:0,}^{1}(Q) \to H_{0,}^{1/2}(\Sigma), \qquad \gamma_{\Sigma}^{i}: H_{:0}^{1}(Q) \to H_{:0}^{1/2}(\Sigma),$$

are continuous and surjective.

2.3 Layer potentials and boundary integral operators

For the sake of clarity, we briefly recall the definition of the *double layer potential* \mathcal{D} from (3):

$$(\mathscr{D}z)(x,t) := \int_0^t \int_{\Gamma} \partial_{n_y} G(x-y,t-\tau) \, z(y,\tau) \, ds_y \, d\tau,$$

for $(x,t) \in Q$ and z a regular enough density. Similarly, we also introduce the single layer potential ${\mathscr S}$

$$(\mathscr{S}w)(x,t) := \int_0^t \int_{\Gamma} G(x-y,t-\tau) \, w(y,\tau) \, ds_y \, d\tau,$$

for $(x,t) \in Q$ and w a regular enough density.

Let γ_N^i be the interior Neumann trace, which is defined variationally as in [10]. Without loss of generality, let us consider $\Omega^c := B_R \setminus \overline{\Omega}$ and $Q^c := \Omega^c \times (0,T)$, with $B_R := \{\mathbf{x} \in \mathbb{R}^n : |\mathbf{x}| < R\}$ a sufficiently large ball containing Γ . This allows us to define the exterior traces γ_{Σ}^e and γ_N^e in analogy to γ_{Σ}^i and γ_N^i , but using Q^c instead of Q. With this, we can define the BIOs in the classical way as [11, Sec. 4]

 $\begin{aligned} \text{Weakly singular operator}: & \qquad \forall \ w := \gamma_{\Sigma}^{i} \mathscr{S}w = \gamma_{\Sigma}^{e} \mathscr{S}w; \\ \text{Double layer operator}: & \qquad \mathsf{K} \ z := \frac{1}{2} \left(\gamma_{\Sigma}^{i} \mathscr{D}z + \gamma_{\Sigma}^{e} \mathscr{D}z \right); \\ \text{Adjoint double layer operator}: & \qquad \mathsf{K}' \ w := \frac{1}{2} \left(\gamma_{N}^{i} \mathscr{S}w + \gamma_{N}^{e} \mathscr{S}w \right); \\ \text{Hypersingular operator}: & \qquad \mathsf{W} \ z := -\gamma_{N}^{i} \mathscr{D}z = -\gamma_{N}^{e} \mathscr{D}z. \end{aligned}$

As already pointed out, the double layer operator K is the main character in this paper. Therefore, we discuss its properties in the next subsection².

3 Main Results

3.1 Mapping induced by the double layer operator K

We now focus on studying the effect of applying K to a function in our trace space, as this will be needed to prove ellipticity later on.

²and refer the interested reader to [36, Sec. 5] for further details about the other operators

Let $v \in H_{0}^{s}(\Sigma)$ with $s \in [0,1]$, in 1d we can express Kv as:

$$\mathsf{K}\,v(x,t) := \frac{1}{2} \int_{\Sigma} \partial_{\mathbf{n}_y} \mathsf{H}(x-y,t-\tau) v(y,\tau) ds_y d\tau, \quad (x,t) \in \Sigma, \tag{8}$$

with $\partial_{\mathbf{n}_y}$ the normal derivative with respect to y.

Let $\mathbf{n}(x)$ denote the outward normal vector with respect to Γ at x. Since $\Gamma := \{0, L\}$, we have in this case $\mathbf{n}(0) = -1$ and $\mathbf{n}(L) = 1$. Then, one can verify that

$$\partial_{\mathbf{n}_y} \mathsf{H}(x - y, t - \tau) = \mathbf{n}(y) \operatorname{sign}(x - y) \, \delta(t - \tau - |x - y|), \tag{9}$$

where sign (\cdot) denotes the signum function and $\delta(\cdot)$ the Dirac delta distribution. Combining (8) and (9), we get

$$\mathsf{K}\,v(x,t) = -\frac{1}{2} \int_0^T \mathrm{sign}\,(x)\,\delta(t-\tau-|x|)v(0,\tau)\,d\tau \\ + \frac{1}{2} \int_0^T \mathrm{sign}\,(x-L)\,\delta(t-\tau-|x-L|)v(L,\tau)\,d\tau. \tag{10}$$

Since sign(0) = 0, we can further reduce (10) to

$$\mathsf{K}\,v(x,t) = \begin{cases} -\frac{1}{2}v(L,t-L) & x = 0, \\ -\frac{1}{2}v(0,t-L) & x = L. \end{cases}, \quad \text{for } v \in H^s_{0,}(\Sigma), \, s \in [0,1]. \tag{11}$$

Remark 3.1. We gather from (11) that the application of K to a function v simply translates v in time and flips its position in space by interchanging the evaluation on x = 0 by x = L, and vice-versa. We will exploit this when we prove ellipticity.

3.2 Continuity and ellipticity in $L^2(\Sigma)$

Using (11), we have that:

$$\left(\pm \frac{1}{2}\operatorname{Id} + \mathsf{K}\right)w(x,t) := \begin{cases} \pm \frac{1}{2}w(0,t) - \frac{1}{2}w(L,t-L) & x = 0 \\ \pm \frac{1}{2}w(L,t) - \frac{1}{2}w(0,t-L) & x = L. \end{cases}$$

Since we focus on second-kind formulations (4) and (5), we need to understand where these BIEs make sense. Let us begin with the scenario when the Dirichlet data g is in $L^2(\Sigma)$. Since we are interested in the Dirichlet problems (1)- (2), let us consider $w \in L^2(\Sigma)$ such that $w(\cdot,t) = 0$ for all $t \leq 0$. Then, for $t \leq L$ we get

$$\left\| \left(\pm \frac{1}{2} \operatorname{Id} + \mathsf{K} \right) w \right\|_{L^2(\Sigma)} \leq \left\| \pm \frac{1}{2} w \right\|_{L^2(\Sigma)} \leq \frac{1}{2} \left\| w \right\|_{L^2(\Sigma)},$$

while for t > L

$$\left\| \left(\pm \frac{1}{2} \operatorname{Id} + \mathsf{K} \right) w \right\|_{L^2(\Sigma)} \leq \left\| \pm \frac{1}{2} w \right\|_{L^2(\Sigma)} + \left\| -\frac{1}{2} w(\cdot, t-L) \right\|_{L^2(\Sigma)} \leq \left\| w \right\|_{L^2(\Sigma)}.$$

Hence, we have continuity of the operators $\left(\pm \frac{1}{2}\operatorname{Id} + \mathsf{K}\right): L^2(\Sigma) \to L^2(\Sigma)$. To show ellipticity in $L^2(\Sigma)$, we will follow the proof of Theorem 2.1 in [37]. For this, we introduce

$$n := \min \Big\{ m \in \mathbb{N} : T \le mL \Big\}, \tag{12}$$

which is the number of time slices $T_j := ((j-1)L, jL)$ for j = 1, ..., n in the case T = nL. In the case T < nL, we define the last time slice as $T_n := ((n-1)L, T)$, while all the others remain unchanged.

Theorem 3.2. For all $w \in L^2(\Sigma)$, there holds the ellipticity estimate

$$\left| \left(\left(\pm \frac{1}{2} \operatorname{Id} + \mathsf{K} \right) w, w \right)_{L^{2}(\Sigma)} \right| \geq c_{s}(n) \left\| w \right\|_{L^{2}(\Sigma)}^{2}, \tag{13}$$

where the number $n \in \mathbb{N}$ of time slices is defined in (12), and

$$c_s(n) := \sin^2\left(\frac{\pi}{2(n+1)}\right) \quad n \ge 1. \tag{14}$$

Proof. When $t \leq L$, we have that

$$\left| \left(\left(\pm \frac{1}{2} \operatorname{Id} + \mathsf{K} \right) w, w \right)_{L^{2}(\Sigma)} \right| = \left| \pm \frac{1}{2} \left(w, w \right)_{L^{2}(\Sigma)} \right| = \frac{1}{2} \left\| w \right\|_{L^{2}(\Sigma)}^{2}, \tag{15}$$

so the operator is $L^2(\Sigma)$ - elliptic with constant $\frac{1}{2}$.

Let T_j denote the j-th time-slice, $j=1,\ldots,n$. Clearly, t>L implies that we assume n>1. Given $w\in L^2(\Sigma)$:

$$\begin{split} \left| 2 \left(\left(\pm \frac{1}{2} \operatorname{Id} + \mathsf{K} \right) w \,,\, w \right)_{L^2(\Sigma)} \right| &= \left| 2 \left(\left(\frac{1}{2} \operatorname{Id} \pm \mathsf{K} \right) w \,,\, w \right)_{L^2(\Sigma)} \right| \\ &= \left| \left\| w(0,\cdot) \right\|_{L^2(\Sigma)}^2 + \left\| w(L,\cdot) \right\|_{L^2(\Sigma)}^2 \\ &\mp \int_{\Sigma} w(L,t) w(0,t-L) \;dt \\ &\mp \int_{\Sigma} w(0,t) w(L,t-L) \;dt \right|. \end{split}$$

Now, we notice this is the same we had in the proof of Theorem 2.1 in [37, page

4]. We therefore use the same computations derived there to get the following:

$$\begin{split} & \left| 2 \left(\left(\frac{1}{2} \operatorname{Id} \pm \mathsf{K} \right) w \,, \, w \right)_{L^2(\Sigma)} \right| \\ & = \left| \sum_{j=1}^n \left[\left\| w(0, \cdot) \right\|_{L^2(T_j)}^2 + \left\| w(L, \cdot) \right\|_{L^2(T_j)}^2 \right. \\ & \left. \mp \int_{T_j} w(L, t) w(0, t - L) \,\, dt \, \mp \int_{T_j} w(0, t) w(L, t - L) \,\, dt \right] \right| \\ & \geq \left| \sum_{j=1}^n \left[\left\| w(0, \cdot) \right\|_{L^2(T_j)}^2 + \left\| w(L, \cdot) \right\|_{L^2(T_j)}^2 \right] \\ & - \sum_{j=2}^n \left[\left\| w(0, \cdot) \right\|_{L^2(T_j)} \left\| w(L, \cdot) \right\|_{L^2(T_{j-1})} + \left\| w(L, \cdot) \right\|_{L^2(T_j)} \left\| w(0, \cdot) \right\|_{L^2(T_{j-1})} \right] \\ & \geq \sum_{j=1}^n \left[\left\| w(0, \cdot) \right\|_{L^2(T_j)}^2 + \left\| w(L, \cdot) \right\|_{L^2(T_{j-1})} + \left\| w(L, \cdot) \right\|_{L^2(T_j)} \left\| w(0, \cdot) \right\|_{L^2(T_{j-1})} \right] \\ & \geq 2 \sin^2 \frac{\pi}{2(n+1)} \left\| w \right\|_{L^2(\Sigma)}^2, \end{split}$$

which shows the ellipticity of $\left(\pm \frac{1}{2} \operatorname{Id} + \mathsf{K}\right)$ in $L^2(\Sigma)$ with ellipticity constant $c_s(n) := \sin^2 \frac{\pi}{2(n+1)}$.

By Lax-Milgram, the continuity and ellipticity in L^2 implies that (4) and (5) have unique solutions. Moreover, by choosing a conforming discretisation, we will also get unique solvability of the arising linear system.

3.3 Existence and uniqueness in $H_{0}^{1}(\Sigma)$ and $H_{0}^{1/2}(\Sigma)$

We first turn our attention to the scenario when the Dirichlet data g is in $H_{0,}^{1}(\Sigma)$, although ultimately, what we truly aim for is the case $g \in H_{0,}^{1/2}(\Sigma)$. With this purpose in mind, we obtain the following result:

Theorem 3.3. In 1d, the operators $\pm \frac{1}{2} \operatorname{Id} + \operatorname{K} : H_{0,}^{1}(\Sigma) \to H_{0,}^{1}(\Sigma)$ are continuous and isomorphisms.

Proof.

<u>Step 1:</u> We begin by recalling from [21, Thm. 20] that W satisfies the ellipticity estimate

$$\langle \mathsf{W}\,\phi\,,\,\partial_t\phi\rangle_\Sigma \geq c(T)\left\|\partial_t\phi\right\|_{L^2(\Sigma)}^2,\quad \forall \phi\in H^1_{0,1}(\Sigma),$$

for some constant c(T) > 0 depending on the terminal time T. The fact that $\partial_t : H^1_{0,}(\Sigma) \to L^2(\Sigma)$ is an isomorphism [37, p. 6] implies the existence of its inverse, which we denote by ∂_t^{-1} .

By taking $v = \partial_t^{-1} \phi$, for $\phi \in H_0^1(\Sigma)$ we obtain

$$\langle \mathsf{W} \, \partial_t^{-1} v \,, \, v \rangle_{\Sigma} \ge c(T) \, \|v\|_{L^2(\Sigma)}^2 \,, \quad \forall v \in L^2(\Sigma),$$

i.e., $\mathsf{W}\,\partial_t^{-1}:L^2(\Sigma)\to L^2(\Sigma)$ defines an isomorphism. Hence $\mathsf{W}:H^1_{0,}(\Sigma)\to L^2(\Sigma)$ is also an isomorphism.

<u>Step 2:</u> Finally, using that in $1d \vee : L^2(\Sigma) \to H_{0,}^1(\Sigma)$ is continuous and an isomorphism, as shown in [37, Sec. 2], we conclude the desired result from the Calderón identity [36, p. 18]

$$VW = \left(\frac{1}{2}\operatorname{Id} - K\right)\left(\frac{1}{2}\operatorname{Id} + K\right). \tag{16}$$

Similarly, we can prove:

Theorem 3.4. In 1d, the operators $\pm \frac{1}{2}\operatorname{Id} + \operatorname{K}: H_{0,}^{1/2}(\Sigma) \to H_{0,}^{1/2}(\Sigma)$ are continuous and isomorphisms.

Proof.

<u>Step 1:</u> By step 1 in the proof of Theorem 3.3, we have that $W: H_{0,}^{1}(\Sigma) \to L^{2}(\Sigma)$ is an isomorphism.

<u>Step 2:</u> By duality, we get that $W: L^2(\Sigma) \to [H^{1}_{,0}(\Sigma)]'$ is an isomorphism. Hence, by interpolation, $W: H^{1/2}_{0,}(\Sigma) \to [H^{1/2}_{,0}(\Sigma)]'$ is also an isomorphism. <u>Step 3:</u> Finally, we proceed as in step 1 in the proof of Theorem 3.3, but now using that in $1d \ V: [H^{1/2}_{,0}(\Sigma)]' \to H^{1/2}_{0,}(\Sigma)$ is continuous and an isomorphism, as shown in [37, Sec. 2].

Theorems 3.3 and 3.4 imply that the operators satisfy their corresponding inf-sup conditions, which would be enough to have existence and uniqueness for the related boundary integral equations of the second kind. Yet, they will not suffice to guarantee that we satisfy the required discrete inf-sup conditions. This will be addressed in the next Section.

4 Discretisation

Let Σ_h be a mesh of the lateral boundary Σ , consisting of non-overlapping intervals and with maximal meshwidth h. Furthermore, we assume the spatial part of the support of each element is restricted to either the left (x=0) or the right (x=L) boundary. In other words, we can write $\Sigma_h = \Sigma_h^0 \cup \Sigma_h^L$, with Σ_h^0 a partition of the left boundary $\{x=0\} \times (0,T)$, and Σ_h^L a partition of the right boundary $\{x=L\} \times (0,T)$.

We consider the following boundary element spaces

- $\mathcal{S}^0(\Sigma_h)$ that is spanned by space-time piecewise constant basis functions on Σ_h ;
- $S_{0}^{1}(\Sigma_{h})$ that is spanned by space-time piecewise linear basis functions on Σ_{h} with zero-initial conditions.

As stated in Theorem 3.2, the operator $-\frac{1}{2}\operatorname{Id} + K$ is continuous and elliptic in $L^2(\Sigma)$. Hence, for given Dirichlet data $g_D \in L^2(\Sigma)$, we the following conforming Galerkin formulation will be uniquely solvable:

Find
$$z_h^0 \in \mathcal{S}^0(\Sigma_h)$$
 such that
$$\left(\left(-\frac{1}{2}\operatorname{Id} + \mathsf{K}\right)z_h^0, q_h\right)_{L^2(\Sigma)} = (g_D, q_h)_{L^2(\Sigma)}, \tag{17}$$
for all $q_h \in \mathcal{S}^0(\Sigma_h) \subset L^2(\Sigma)$.

Additionally, inspired by Theorem 3.4, we pursue the following Galerkin discretisation of (4):

Find
$$z_h^1 \in \mathcal{S}_{0,}^1(\Sigma_h) \subset H_{0,}^{1/2}(\Sigma)$$
 such that
$$\left\langle \left(-\frac{1}{2} \operatorname{Id} + \mathsf{K} \right) z_h^1, v_h \right\rangle_{\Sigma} = \langle g, v_h \rangle_{\Sigma},$$
for all $v_h \in \mathcal{S}_{0,}^1(\Sigma_h) \subset [H_{0,}^{1/2}(\Sigma)]'.$ (18)

Note that our results from Section 3 also allow us to consider (18) in $H_{0,}^{1}(\Sigma)$, but omit it for conciseness.

We obviously proceed analogously for (5), but we will refrain from writing the formula for the sake of brevity. In order to have stability, we need to introduce one requirement on the family of meshes that we can use:

Definition 4.1. Let X_h be a boundary element space. A mesh Σ_h of Σ is X_h -admissible if the L^2 -orthogonal projection onto X_h is H^1 -stable.

Remark 4.2. The H^1 -stability in Definition 4.1 is a well studied requirement in Galerkin discretisations. It always holds for globally quasi-uniform meshes and piecewise polynomial finite element spaces [7, 34] (and hence in particular for

 $S^1(\Sigma_h)$). For locally refined meshes, one needs to (i) impose a-priori bounds on the gradings of the mesh, as in [6, 8, 13, 15, 29]; (ii) impose a fixed refinement strategy [4, 9, 27]; or (iii) a combination of both [28, 20].

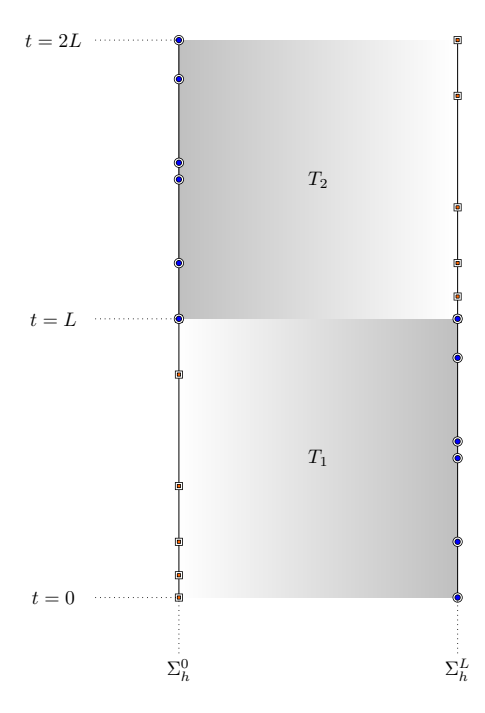


Figure 1: Example of non-uniform mesh satisfying Assumption 4.3. On each time-slice T_j , the degrees of freedom (DoFs) of each boundary agree with the DoFs on the opposite boundary shifted in time by L.

In order to ensure discrete inf-sup stability, we impose some additional constraints on the $S_{0,}^{1}(\Sigma_{h})$ -admissible mesh. We assume the following mesh condition holds:

Assumption 4.3. Let us assume T = nL for some $n \in \mathbb{N}$ and consider the time-slices $T_j := ((j-1)L, jL)$ for j = 1, ..., n. Let Σ_h be mesh of Σ . We further assume that the mesh on the boundary restricted to a time-slice corresponds to the mesh on the opposite boundary restricted to the subsequent time-slice. In other words, we require:

$$\Sigma_{h|T_j}^0 = \Sigma_{h|T_{j+1}}^L$$
, and $\Sigma_{h|T_j}^L = \Sigma_{h|T_{j+1}}^0$, $\forall j = 1, \dots, n-1$. (19)

Clearly, all uniform meshes satisfy this assumption. An example of a non-uniform mesh satisfying assumption 4.3 is given in Figure 1.

Then, we can show the following result:

Theorem 4.4. Let Σ_h be an $\mathcal{S}^1_{0,}(\Sigma_h)$ -admissible mesh of Σ such that Assumption 4.3 holds. Then, the following discrete inf-sup conditions are satisfied in 1d

$$c_{1}^{\mathsf{K}} \| w_{h} \|_{H_{0,}^{1/2}(\Sigma)} \leq \sup_{0 \neq \mu_{h} \in \mathcal{S}_{0}^{1}(\Sigma_{h})} \frac{\left| \left\langle \left(\pm \frac{1}{2} \operatorname{\mathsf{Id}} + \mathsf{K} \right) w_{h}, \mu_{h} \right\rangle_{\Sigma} \right|}{\| \mu_{h} \|_{[H_{0}^{1/2}(\Sigma)]'}}, \tag{20}$$

for all $w_h \in \mathcal{S}_{0,}^1(\Sigma_h)$.

We dedicate the remaining of this subsection to prepare the required ingredients to prove this Theorem.

4.1 Proof of Theorem 4.4

We begin by introducing the L^2 projection $Q_h^0: L^2(\Sigma) \to \mathcal{S}_{0,}^1(\Sigma_h)$ as

$$\langle Q_h^0 u, v_h \rangle_{\Sigma} = \langle u, v_h \rangle_{\Sigma}, \quad \forall v_h \in \mathcal{S}_{0}^1(\Sigma_h).$$
 (21)

Let $Q_h^{0*}: L^2(\Sigma) \to \mathcal{S}_{0,}^1(\Sigma_h) \subset L^2(\Sigma)$ be the unique (Hilbert space-)adjoint operator. We note that in this case $Q_h^{0*} = Q_h^0$.

In order to proceed, we need to show the following auxiliary result

Lemma 4.5. For $S_{0}^{1}(\Sigma_{h})$ -admissible meshes

$$\|Q_h^0 \nu\|_{[H_0^{1/2}(\Sigma)]'} \le c_s \|\nu\|_{[H_0^{1/2}(\Sigma)]'}, \qquad \forall \nu \in [H_0^{1/2}(\Sigma)]',$$
 (22)

is satisfied with a constant $c_s > 0$.

Proof. We have that

$$\left\|Q_h^0 w\right\|_{L^2(\Sigma)} \le \left\|w\right\|_{L^2(\Sigma)}, \qquad \forall w \in L^2(\Sigma), \tag{23}$$

and, from the definition of $\mathcal{S}_0^1(\Sigma_h)$ -admissibility, that

$$\|Q_h^0 w\|_{H_0^1(\Sigma)} \le c_{s,1} \|w\|_{H_{0,1}^1(\Sigma)}, \quad \forall w \in H_{0,1}^1(\Sigma).$$
 (24)

Hence, by interpolation of bounded linear operators, we get that

$$\|Q_h^0 w\|_{H_0^{1/2}(\Sigma)} \le \sqrt{c_{s,1}} \|w\|_{H_0^{1/2}(\Sigma)}, \quad \forall w \in H_0^{1/2}(\Sigma).$$
 (25)

Moreover, by [34, Theorem 2.1], this is equivalent to

$$\|Q_h^{0*}\nu\|_{[H_0^{1/2}(\Sigma)]'} \le \sqrt{c_{s,1}} \|\nu\|_{[H_0^{1/2}(\Sigma)]'}, \qquad \forall \nu \in [H_0^{1/2}(\Sigma)]', \tag{26}$$

Finally, the result follows from $Q_h^{0*}=Q_h^0$ in our case.

Now we have all the pieces to show our main theorem.

Proof of Theorem 4.4. Without loss of generality, let us prove our result for $\left(-\frac{1}{2}\operatorname{Id} + \mathsf{K}\right)$ and note that $\left(\frac{1}{2}\operatorname{Id} + \mathsf{K}\right)$ follows analogously. From [36, Thm. 5.6] we know that $\left(\frac{1}{2}\operatorname{Id} - \mathsf{K}\right)$ satisfies the continuous inf-sup condition, we henceforth can pick a $\mu_w \in [H_0^{1/2}(\Sigma)]'$ such that

$$\frac{\left|\left\langle \left(-\frac{1}{2}\operatorname{Id} + \mathsf{K}\right)w, \, \mu_{w}\right\rangle_{\Sigma}\right|}{\|\mu_{w}\|_{[H_{0}^{1/2}(\Sigma)]'}} \ge \alpha_{\mathsf{K}} \|w\|_{H_{0,-}^{1/2}(\Sigma)}, \quad \forall w \in H_{0,-}^{1/2}(\Sigma), \tag{27}$$

for some $0 < \alpha_{\mathsf{K}} < \infty$.

Let $w_h \in \mathcal{S}_{0,}^1(\Sigma_h)$. Note that $w_h \in H_{0,}^{1/2}(\Sigma)$, hence (27) holds with a $\mu_{w_h} \in [H_{0,}^{1/2}(\Sigma)]'$. In general, given the mapping properties of K (see (11)), we cannot assume K $w_h \in \mathcal{S}_{0,}^1(\Sigma_h)$. Nevertheless, as K induces a translation in time of magnitude L, the function K w_h remains piecewise linear, and Assumption 4.3 guarantees that $(-\operatorname{Id} + \operatorname{K})w_h \in \mathcal{S}_{0,}^1(\Sigma_h)$.

Considering this, we derive

$$\begin{split} \sup_{0 \neq \mu_h \in \mathcal{S}_{0,}^{1}(\Sigma_h)} \frac{\left| \left\langle \left(-\frac{1}{2} \operatorname{Id} + \mathsf{K} \right) w_h \,,\, \mu_h \right\rangle_{\Sigma} \right|}{\|\mu_h\|_{[H_{0,}^{1/2}(\Sigma)]'}} &\geq \frac{\left| \left\langle \left(-\frac{1}{2} \operatorname{Id} + \mathsf{K} \right) w_h \,,\, Q_h^0 \mu_{w_h} \right\rangle_{\Sigma} \right|}{\|Q_h^0 \mu_{w_h}\|_{[H_{0,}^{1/2}(\Sigma)]'}} \\ &\stackrel{(26)}{\geq} \frac{\left| \left\langle \left(-\frac{1}{2} \operatorname{Id} + \mathsf{K} \right) w_h \,,\, Q_h^0 \mu_{w_h} \right\rangle_{\Sigma} \right|}{c_s \, \|\mu_{w_h}\|_{[H_{0,}^{1/2}(\Sigma)]'}} \\ &\stackrel{(21)}{=} \frac{\left| \left\langle \left(-\frac{1}{2} \operatorname{Id} + \mathsf{K} \right) w_h \,,\, \mu_{w_h} \right\rangle_{\Sigma} \right|}{c_s \, \|\mu_{w_h}\|_{[H_{0,}^{1/2}(\Sigma)]'}} \\ &\stackrel{\text{Thm. } 3.4}{\geq} \frac{\alpha_{\mathsf{K}}}{c_s} \, \|w_h\|_{H_{0,}^{1/2}(\Sigma)}, \end{split}$$

for all $w_h \in \mathcal{S}_{0,}^1(\Sigma_h)$, which proves the theorem with $c_1^{\mathsf{K}} = \frac{\alpha_{\mathsf{K}}}{c_s}$.

5 Error Estimates

Based on standard arguments [31, 35], we derive a priori error estimates for the Galerkin approximations (17) and (18).

As a consequence of Theorem 4.4 and [31, Thm. 4.2.1], we have that:

Proposition 5.1. Let $z \in H_{0,}^{1/2}(\Sigma)$ be the exact solution to (5) and $z_h^1 \in \mathcal{S}_{0,}^1(\Sigma_h)$ the discrete solution of (18). The following a priori error estimate holds

$$||z - z_h^1||_{H_{0,}^{1/2}(\Sigma)} \le \left(1 + \frac{||\pm \frac{1}{2} \operatorname{Id} + \mathsf{K}||}{c_1^{\mathsf{K}}}\right) \inf_{v_h \in \mathcal{S}_{0,}^1(\Sigma_h)} ||z - v_h||_{H_{0,}^{1/2}(\Sigma)}, \tag{28}$$

where c_1^{K} is the inf-sup constant from (20).

Combining Proposition 5.1 with the approximation property of the space of piecewise linear functions [35, Thm. 10.9], yields the a priori error estimate:

Corollary 5.2. Let $z \in H_{0,}^{s}(\Sigma)$ for $s \in [1/2, 2]$ denote the exact solution to (4). Then for the Galerkin solution $z_{h}^{1} \in \mathcal{S}_{0}^{1}(\Sigma_{h})$ we have the a priori error estimate

$$||z - z_h^1||_{H_{0.}^{1/2}(\Sigma)} \le \tilde{c} \, h^{s-1/2} \, ||z||_{H^s(\Sigma)} \,, \tag{29}$$

for a positive constant \tilde{c} independent of h.

Similarly, by Theorem 3.2, we can use the standard tools for elliptic problems and the approximation property of the space of piecewise constants [35, Thm. 10.4] to get

Corollary 5.3. Let $z \in H_{0,}^{s}(\Sigma)$ for $s \in [0,1]$ denote the exact solution to (4). Then for the Galerkin solution $z_{h}^{0} \in \mathcal{S}^{0}(\Sigma_{h})$ we have the a priori error estimate

$$||z - z_h^0||_{L^2(\Sigma)} \le \tilde{c}_0 h^s ||z||_{H^s(\Sigma)},$$
 (30)

for a positive constant \tilde{c}_0 independent of h.

6 Numerical Experiments

Before we present our numerical results, we dedicate the next two subsections to briefly describe a couple of tools that we will use.

6.1 Norm approximation

The error is measured in the $H_{0,}^{1/2}(\Sigma)$ -norm, which can be represented using the modified Hilbert transform \mathcal{H}_T [38, Section 2.4]:

$$\langle \partial_t u, \mathcal{H}_T u \rangle_{\Sigma} = \|u\|_{H_{0,\cdot}^{1/2}(\Sigma)}^2, \quad \text{for all } u \in H_{0,\cdot}^{1/2}(\Sigma).$$

Computation of the $H_{0,}^{1/2}(\Sigma)$ requires a representation of the functions $\mathcal{H}_T z$, where z is the exact solution of (4). As these terms are often challenging to retrieve, we approximate the $H_{0,}^{1/2}(\Sigma)$ -norm by interpolating z. Since the exact solutions we will consider for our experiments are globally continuous, we are allowed to define the interpolation of z by using the (standard) nodal interpolation operator $I_h: C^0(\Sigma) \to \mathcal{S}_{0,}^1(\Sigma_h)$.

It is worth pointing out that the expected convergence rate of the Galerkin approximation is not affected by the interpolation of the exact solution, and therefore this will not affect our numerical results.

6.2 Exact representation of the unknown density

In general, solutions to the indirect methods do not yield densities which can be interpreted physically. This limits the possibility to find an exact representation of the density, solving (4). However, if the following assumption holds on the Dirichlet data

$$g(0, t - NL) = g(L, t - (N - 1)L), \quad N \in \mathbb{N}, \ t \ge 0, \tag{31}$$

an exact solution is available. In order to see this, let us first restate the considered BIE, assuming a positive addition of the double layer operator

$$\left(-\frac{1}{2}\operatorname{Id} + \mathsf{K}\right)z = g.$$

Next, let us consider the candidate solution \bar{z} defined as

$$\bar{z}(x,t) := \begin{cases} -2 \ g(L,t+L) & x = 0\\ 0 & x = L. \end{cases}$$
 (32)

Then, by (11), we have

$$\mathsf{K}\,\bar{z} := \begin{cases} 0 & x = 0\\ g(L, t) & x = L. \end{cases} \tag{33}$$

Now, the full equation reads

$$\left(-\frac{1}{2}\operatorname{Id} + \mathsf{K}\right)\bar{z} = \begin{cases} g(L, t+L) & x = 0, \\ g(L, t) & x = L, \end{cases}$$
(34)

which, given the assumption (31) results in

$$\left(-\frac{1}{2}\operatorname{Id} + \mathsf{K}\right)\bar{z} = \begin{cases} g(0,t) & x = 0, \\ g(L,t) & x = L. \end{cases}$$
(35)

Hence, \bar{z} is the unique solution to (4).

6.3 Numerical results

Our code is implemented in PYTHON. We use exact integration to obtain the entries of the Galerkin matrix, while we resort to built-in quadrature routines (SCIPY.INTEGRATE.QUAD) to compute the right-hand side of the system. The resulting linear systems of equations are solved using a built-in direct solver (NumPy.Linalg.solve).

We point out that it suffices to test the interior problem since the only difference between (4) and (5) is the sign of the identity, whose discretisation is stable under our assumptions and choice of boundary element spaces. We first

validate our theoretical results with $\Omega := (0,3)$, T = 6, and the following exact solutions for (1), which are also used in [37]:

$$u_a(x,t) = \begin{cases} \frac{1}{2}(t-x-2)^3(t-x)^3 & x \le t \le 2+x, \\ 0 & \text{else.} \end{cases}$$
 (36)

$$u_b(x,t) = \begin{cases} \frac{1}{2} |\sin(\pi(x-t))|, & x \le t, \\ 0 & \text{else.} \end{cases}$$
 (37)

Our Dirichlet data is obtained by taking the lateral trace on either (36) or (37). Since in both cases, it satisfies assumption (31), we are able to find an expression for the exact solution to the unknown density, following the cue of subsection 6.2.

We measure the corresponding error for each experiment and the condition number κ for the Galerkin matrix corresponding to $-\frac{1}{2}\operatorname{Id}+\mathsf{K}$. First we consider a set of uniform meshes.

6.3.1 Piecewise constant discretisation

First we consider the numerical approximation in $L^2(\Sigma)$, considering the Galerkin formulation (17). The results are presented in Table 1, where N denotes the number of elements used to discretise the lateral boundary Σ_h and eoc stands for estimated order of convergence. Let z_a and z_b be the exact solutions to (4) with Dirichlet data corresponding to (36) and (37) respectively. Additionally, we denote the obtained numerical solutions by $z_{a,h}^0$ and $z_{b,h}^0$. We observe that for both experiments, the expected convergence rate is achieved. Fun fact: the resulting condition number corresponds exactly with the golden ratio squared.

Table 1: Numerical results for (4) in L^2 using $S^0(\Sigma_h)$. Given Dirichlet data corresponding to solutions (36), and (37) and when using uniform meshes.

N	$\left\ z_a - z_{a,h}^0 \right\ _{L^2(\Sigma)}$	eoc	$\left\ z_b - z_{b,h}^0\right\ _{L^2(\Sigma)}$	eoc	κ
64	8.77E-02	1	2.70E-01	1	2.62E+00
128	4.41E-02	0.99	1.42E-01	0.93	2.62E+00
256	2.21E-02	1.0	7.22E-02	0.97	2.62E+00
512	1.10E-02	1.0	3.65E-02	0.99	2.62E+00
1024	5.52E-03	1.0	1.83E-02	0.99	2.62E+00
2048	2.76E-03	1.0	9.18E-03	1.0	2.62E+00

6.3.2 Piecewise linear discretisation

The results related to (18) are displayed in Table 2, where N denotes the number of elements used to discretise the lateral boundary Σ_h . Like in the piecewise

constant case, we let z_a and z_b be the exact solutions to (4) with Dirichlet data corresponding to (36) and (37) respectively. Furthermore, we denote the obtained numerical solutions by $z_{a,h}^1$ and $z_{b,h}^1$. Expected convergence rate is achieved, leading to higher or equal rate compared to the piecewise constant discretisation.

Table 2: Numerical results for (4) in $H_{0,}^{1/2}(\Sigma)$ using $\mathcal{S}_{0,}^{1}(\Sigma_{h})$. Given Dirichlet data corresponding to solutions (36), and (37) and when using uniform meshes.

N	$\left\ I_h z_a - z_{a,h}^1\right\ _{H_{0,\cdot}^{1/2}(\Sigma)}$	eoc	$\left\ I_h z_b - z_{b,h}^1\right\ _{H_{0,}^{1/2}(\Sigma)}$	eoc	κ
64	4.34E-02	-	3.91E-01	-	8.09E+00
128	1.47E-02	1.57	1.88E-01	1.06	8.12E+00
256	5.10E-03	1.52	9.22E-02	1.03	8.12E + 00
512	1.79E-03	1.51	4.57E-02	1.01	8.13E+00
1024	6.33E-04	1.5	2.28E-02	1.01	8.13E+00
2048	2.24E-04	1.5	1.13E-02	1.01	8.13E+00

Next, we rerun the experiments on a family of meshes which do not meet Assumption 4.3. In order to achieve this, we consider a terminal time $T=2\pi$ and L=3, ensuring that on each boundary no uniform refinement will lead to vertices at intersections between time-slices. Moreover, the boundaries at x=0 and x=L are divided into N_0 and N_L elements respectively, where we impose $N_0 \neq N_L$. Consider an initial mesh with $N_0=40$ and $N_L=24$. We create the family of meshes by uniformly refining the initial mesh, which is displayed in Figure 2.

The results are given in Table 3. We again observe the expected convergence rate in spite of the fact that our meshes violate Assumption 4.3.

Table 3: Numerical results for (4) given Dirichlet data corresponding to solutions (36) and (37), and using a family of meshes not meeting Assumption T = nL for some $n \in \mathbb{N}$., with $N = N_0 + N_L$.

N	$\left\ I_h z_a - z_{a,h}^1\right\ _{H_{0,\cdot}^{1/2}(\Sigma)}$	eoc	$\left\ I_h z_b - z_{b,h}^1\right\ _{H_{0,}^{1/2}(\Sigma)}$	eoc	κ
64	3.26E-02	-	3.41E-01	-	9.10E+00
128	1.12E-02	1.55	1.80E-01	0.93	9.96E+00
256	3.90E-03	1.52	8.47E-02	1.08	1.03E+01
512	1.37E-03	1.51	3.88E-02	1.13	9.99E+00
1024	4.85E-04	1.5	2.17E-02	0.84	1.04E+01
2048	1.71E-04	1.5	1.08E-02	1.01	1.02E+01

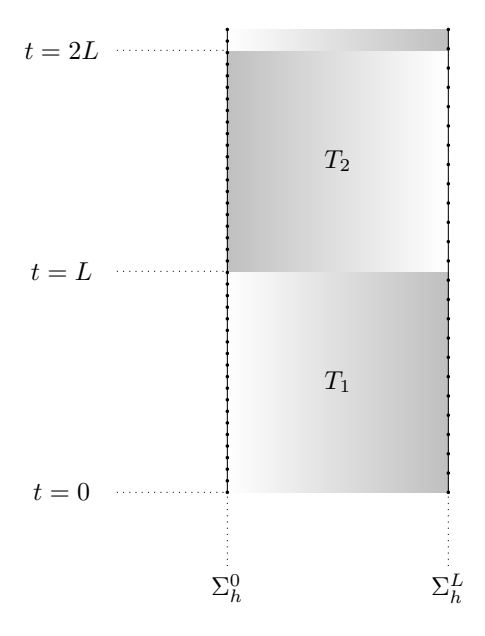


Figure 2: Initial non-uniform mesh which does not satisfy assumption T = nL for some $n \in \mathbb{N}$.

6.3.3 Discrete inf-sup constant

In light of the results from Table 3, we want to understand if the convergence we observed was "a lucky strike" or if we have discrete stability regardless of Assumption 4.3. We do this by checking numerically the obtained discrete infsup constant and whether it remains constant with mesh refinement.

We compute the discrete inf-sup constant following the approach in [25, Rem. 3.159]. In the case of computing the discrete inf-sup constant in $H_{0,}^{1/2}(\Sigma)$, we require the following mass matrix

$$M_y[i,j] = (\psi_i, \psi_j)_{[H_0^{1/2}(\Sigma)]'},$$
 (38)

where span $\{\psi_i\}_{i=1}^N = \mathcal{S}_{0,}^1(\Sigma_h)$.

Since piecewise linear basis functions are in $L^2(\Sigma)$, we use the following equivalence

$$(\psi_i, \psi_j)_{[H_0^{1/2}(\Sigma)]'} \equiv -\left\langle \mathcal{H}_T \psi_i, \overline{\partial}_t^{-1} \psi_j \right\rangle_{\Sigma}, \tag{39}$$

where $\overline{\partial}_t^{-1} f(s) := -\int_t^T f(s) \, ds$ for $f \in L^2(\Sigma)$. The proof of (39) can be found in Appendix A.

Let h_0 and h_L denote the mesh-width of uniformly refined left (x = 0) and right (x = L) boundary respectively. As in Section 6.3.2, when computing the inf-sup constant, we distinguish between the cases where the assumption T = nL, with $n \in \mathbb{N}$ does or does not hold. More specifically, we consider: i) a

uniform mesh with T = nL and $h_0 = h_L$; ii) a (non-uniform) mesh with $T = n\pi$ and $h_0 \neq h_L$.

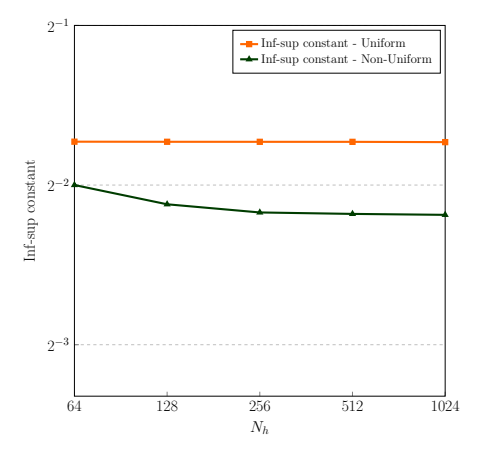


Figure 3: Discrete inf sup constant for different mesh refinements and two types of meshes: the uniform case with T=6; the non-uniform case with $T=2\pi$ and initial mesh given by Figure 2.

Figure 3 displays the discrete inf-sup constant against number of mesh elements. There, we set the final time for the uniform case to T=6, and in the non-uniform case to $T=2\pi$, and increase the level of refinement. We see how the discrete inf-sup constant is asymptotically independent of the mesh-width, which corroborates that the formulation is uniformly discrete inf-sup stable.

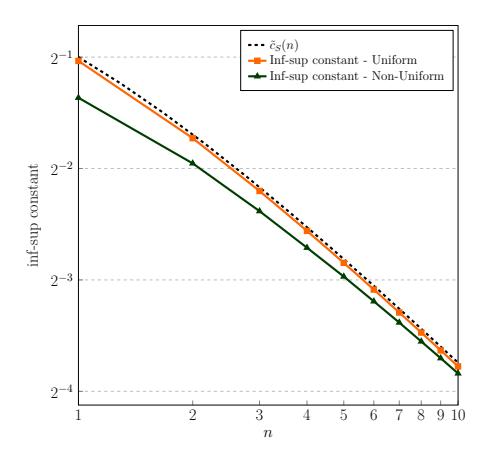


Figure 4: Discrete inf sup constant for different final times: the uniform case with T=nL and $h_0=h_L=3/16$; the non-uniform case with $T=n\pi$ and $h_0=\pi/20$ and $h_L=\pi/12$. Here n is the number of timeslices (and thus refinement independent).

Next, we study numerically how the discrete inf-sup constant depends on the final time T. As shown in Figure 4 the discrete inf-sup constant decreases when the terminal time T increases, yet it remains strictly positive. In case i), the discrete inf-sup constant asymptotically corresponds to the inf-sup constant $\tilde{c}_s(n) = \sin \frac{\pi}{2(2n+1)}$.

7 Conclusion

We presented a simple second-kind formulation for the transient wave equation in 1d that has a proven stable low-order discretisations. We point out that this is the first time that such a result is available without having to resort to a combined field boundary integral operator. It is also a required and insightful first step to achieve the same result for higher spatial-dimensions.

For L^2 the stability will hold for any conforming discretisation, while for $H_0^{1/2}$ we found stable inf-sup pairs. For the proof we required Assumption 4.3, yet we observe in the numerics that this is not needed. Ongoing work is showing stability without this mesh assumption.

It is important to keep in mind that more work is required to generalise the obtained discrete stability to $\Omega \in \mathbb{R}^2$ with d=2,3. In particular, one needs to extend the auxiliary Lemma 4.5 to the space $\mathcal{H}_{0,}(\Sigma)$ defined in [36], since $K:\mathcal{H}_{0,}(\Sigma)\to\mathcal{H}_{0,}(\Sigma)$ in higher dimensions; and to study the mapping properties of the double layer operator K, such that the related projections remain meaningful. The latter result is dimension dependent as a consequence of the fundamental solution being so. For the auxiliary Lemma, however, the density of $H_{0,}^{1/2}(\Sigma)$ in $\mathcal{H}_{0,}(\Sigma)$ is a promising starting point.

We are also cautiously optimistic about the extension of Theorem 3.2 to higher spatial-dimensions. The reason is that, in its proof, one can see how the proposed second kind formulation is connected with energetic BEM for the first kind formulation arising from the weakly singular operator V. Indeed, the infsup constant $c_s(n)$ agrees with the L^2 -ellipticity constant from [1, Theorem 2.1]. Hence, the fact that energetic BEM is known to work in the case of two spatial-dimensions, makes us believe that there is a chance that we can work out the required theory.

Ongoing and future work involves further understanding of the trace spaces \mathcal{H}_0 (Σ) and the BEM implementation in higher dimensions.

References

- [1] A. Aimi, M. Diligenti, C. Guardasoni, I. Mazzieri, and S. Panizzi. An energy approach to space-time Galerkin BEM for wave propagation problems. *Internat. J. Numer. Methods Engrg.*, 80(9):1196–1240, 2009.
- [2] A. Aimi, M. Diligenti, C. Guardasoni, and S. Panizzi. A space-time energetic formulation for wave propagation analysis by BEMs. *Riv. Mat. Univ. Parma* (7), 8:171–207, 2008.

- [3] A. Bamberger and T. Ha Duong. Formulation variationnelle pour le calcul de la diffraction d'une onde acoustique par une surface rigide. *Math. Methods Appl. Sci.*, 8(4):598–608, 1986.
- [4] R. Bank and H. Yserentant. On the H^1 -stability of the L_2 -projection onto finite element spaces. *Numer. Math.*, 126(2):361–381, 2014.
- [5] A. Barnett, L. Greengard, and T. Hagstrom. High-order discretization of a stable time-domain integral equation for 3d acoustic scattering. *Journal* of Computational Physics, 402, 2020.
- [6] J. H. Bramble, J. E. Pasciac, and O. Steinbach. On the stability of the L^2 projection in $H^1(\Omega)$. Mathematics of computation, 71(237):147-156, 2002.
- [7] J. H. Bramble and J. Xu. Some estimates for a weighted L^2 projection. Mathematics of computation, 56(194):463-476, 1991.
- [8] C. Carstensen. Merging the Bramble-Pasciak-Steinbach and the Crouzeix-Thomée criterion for H^1 -stability of the L^2 -projection onto finite element spaces. *Mathematics of Computation*, 71(237):157–163, 2002.
- [9] C. Carstensen. An adaptive mesh-refining algorithm allowing for an H^1 stable L_2 projection onto courant finite element space. Constr. Approx., 20(4):549-564, 2004.
- [10] M. Costabel. Boundary integral operators on Lipschitz domains: elementary results. SIAM J. Math. Anal., 19(3):613–626, 1988.
- [11] M. Costabel. Developments in boundary element methods for time-dependent problems. In *Problems and methods in mathematical physics* (Chemnitz, 1993), volume 134 of Teubner-Texte Math., pages 17–32. Teubner, Stuttgart, 1994.
- [12] M. Costabel and F.-J. Sayas. Time-dependent problems with the boundary integral equation method. In E. Stein, R. Borst, and T. J. R. Hughes, editors, *Encyclopedia of Computational Mechanics Second Edition*. Wiley, 2017.
- [13] M. Crouzeix and V. Thomée. The stability in L_p and W_p^1 of the L_2 Projection onto Finite Element Function Spaces. *Mathematics of computation*, 48(178):521–532, 1987.
- [14] C. L. Epstein, L. Greengard, and T. Hagstrom. On the stability of time-domain integral equations for acoustic wave propagation. DCDS, 36(8):4367-4382, 2016.
- [15] K. Eriksson and C. Johnson. Adaptive finite element methods for parabolic problems. ii. optimal error estimates in $L_{\infty}L_{2}$ and $L_{\infty}L_{\infty}$. SIAM J. Numer. Anal., 32(3):706–740, 1995.

- [16] H. Gimperlein, Z. Nezhi, and E. P. Stephan. A priori error estimates for a time-dependent boundary element method for the acoustic wave equation in a half-space. *Math. Methods Appl. Sci.*, 40(2):448–462, 2017.
- [17] H. Gimperlein, C. Özdemir, D. Stark, and E. P. Stephan. hp-version time domain boundary elements for the wave equation on quasi-uniform meshes. *Comput. Methods Appl. Mech. Engrg.*, 356:145–174, 2019.
- [18] H. Gimperlein, C. Özdemir, D. Stark, and E. P. Stephan. A residual a posteriori error estimate for the time-domain boundary element method. *Numer. Math.*, 146(2):239–280, 2020.
- [19] H. Gimperlein, C. Özdemir, and E. P. Stephan. Time domain boundary element methods for the Neumann problem: error estimates and acoustic problems. *J. Comput. Math.*, 36(1):70–89, 2018.
- [20] H. Gimperlein, J. Stocek, and C. Urzúa-Torres. Optimal operator preconditioning for pseudodifferential boundary problems. *Numer. Math.*, 148:1–41, 2021.
- [21] C. Guardasoni. Wave Propagation Analysis with Boundary Element Method. PhD thesis, University of Milan, 2010.
- [22] T. Ha-Duong. A mathematical analysis of boundary integral equations in the scattering problems of transient waves. *Boundary Element Methods*, 9:101–114, 1987.
- [23] M. E. Hassell, T. Qiu, T. Sánchez-Vizuet, and F.-J. Sayas. A new and improved analysis of the time domain boundary integral operators for the acoustic wave equation. J. Integral Equations Appl., 29(1):107–136, 2017.
- [24] D. Hoonhout, R. Löscher, O. Steinbach, and C. Urzúa-Torres. Stable least-squares space-time boundary element methods for the wave equation. *Arxiv*, 2024. arXiv, 2312.12547v1.
- [25] V. John. Finite Element Methods for Incompressible Flow Problems, volume 51 of Springer Series in Computational Mathematics. Springer, Berlin, 2010.
- [26] P. Joly and J. Rodríguez. Mathematical aspects of variational boundary integral equations for time dependent wave propagation. *J. Integral Equations Appl.*, 29(1):137–187, 2017.
- [27] M. Karkulik, D. Pavlicek, and D. Praetorius. On 2D newest vertex bisection: Optimality of mesh-closure and H^1 -stability of L_2 -projection. Constr. Approx., 38:213–234, 2013.
- [28] M. Karkulik, C. Pfeiler, and D. Praetorius. L^2 orthogonal projections onto finite elements on locally refined meshes are h1 stable. arXiv, 2014. arXiv, 1307.0917v2.

- [29] Steinbach. O. On a generalized L_2 projection and some related stability estimates in sobolev spaces. *Numer. Math.*, 90(4):775–786, 2002.
- [30] D. Pölz and M. Schanz. On the space-time discretization of variational retarded potential boundary integral equations. *Computers & Mathematics with Applications*, 99:195–210, 2021.
- [31] S. Sauter and C. Schwab. Boundary Element Methods. Springer-Verlag, Berlin, Germany, 2010.
- [32] F.-J. Sayas. Energy estimates for Galerkin semidiscretizations of time domain boundary integral equations. *Numer. Math.*, 124(1):121–149, 2013.
- [33] F.-J. Sayas. Retarded potentials and time domain boundary integral equations. A road map, volume 50 of Springer Series in Computational Mathematics. Springer, Cham, 2016.
- [34] O. Steinbach. Stability estimates for hybrid coupled domain decomposition methods, volume 1809 of Lecture Notes in Mathematics. Springer-Verlag, Berlin, 2003.
- [35] O. Steinbach. Numerical approximation methods for elliptic boundary value problems: Finite and boundary elements. Springer, New York, 2008. Finite and boundary elements, Translated from the 2003 German original.
- [36] O. Steinbach and C. Urzúa-Torres. A new approach to space-time boundary integral equations for the wave equation. SIAM Journal on Mathematical Analysis, 54(2):1370–1392, 2022.
- [37] O. Steinbach, C. Urzúa-Torres, and M. Zank. Towards coercive boundary element methods for the wave equation. *J. Integral Equations Appl.*, 34:501–515, 2022.
- [38] O. Steinbach and M. Zank. Coercive space-time finite element methods for initial boundary value problems. *Electron. Trans. Numer. Anal.*, 52:154–194, 2020.

A Representation of the Dual Inner Product

First we recall [37, p. 9] for $u, v \in H_{0}^{1/2}(\Sigma)$

$$\langle \mathcal{H}_T u, \partial_t v \rangle_{\Sigma} = (u, v)_{H_0^{1/2}(\Sigma)}.$$
 (40)

The fact that $\partial_t: H^1_{,0}(\Sigma) \to L^2(\Sigma)$ is an isomorphism [37, p. 6], implies the existence of an inverse operator $\overline{\partial}_t^{-1}: L^2(\Sigma) \to H^1_{,0}(\Sigma)$ which also is an isomorphism. In this case, the inverse operator can be expressed as [37, p. 6]

$$\overline{\partial}_t^{-1} f(s) := -\int_t^T f(s) \, ds, \quad \text{for } f \in L^2(\Sigma). \tag{41}$$

Similarly, the isomorphism $\partial_t: H^1_{0,}(\Sigma) \to L^2(\Sigma)$ has $\partial_t^{-1}: L^2(\Sigma) \to H^1_{0,}(\Sigma)$ as its inverse operator, which is given by

$$\partial_t^{-1} f(s) := -\int_0^t f(s) \, ds, \quad \text{for } f \in L^2(\Sigma).$$
 (42)

Next, we study the properties of $\overline{\partial}_t^{-1}$ properties in the fractional Sobolev spaces under consideration. For this, we need to consider the time derivative in the weak sense.

Lemma A.1. Let $\omega \in [H_{0,}^1(\Sigma)]'$. Then there exists a unique $v \in L^2(\Sigma)$ such that

$$-(v, \partial_t u)_{L^2(\Sigma)} = \langle \omega, u \rangle_{\Sigma} \qquad \forall u \in H^1_{0}(\Sigma), \tag{43}$$

and

$$\|\omega\|_{[H_0^1(\Sigma)]'}^2 = \|v\|_{L^2(\Sigma)}^2. \tag{44}$$

Proof. First, one can show that (43) admits a unique solution $v \in L^2(0,T)$ by using the Babuška–Nečas theory. This implies that $\partial_t : L^2(0,T) \to [H^1_{0,}(0,T)]'$ is an isomorphism. Then, we can derive the following

$$\begin{split} \|\omega\|_{[H^1_{0,}(0,T)]'} &= \sup_{u \in H^1_{0,}(0,T) \setminus \{0\}} \frac{\left| \langle \omega \,,\, u \rangle_{(0,T)} \right|}{\|\partial_t u\|_{L^2(0,T)}} \\ &= \sup_{u \in H^1_{0,}(0,T) \setminus \{0\}} \frac{\left| -(v,\partial_t u)_{L^2(\Sigma)} \right|}{\|\partial_t u\|_{L^2(0,T)}} \leq \|v\|_{L^2(0,T)} \,. \end{split}$$

Next, let us, consider $\bar{u}(t) = \int_0^t v(s) ds$, which satisfies $\partial_t \bar{u} = v$ in $L^2(0,T)$. With this, we arrive to

$$\|v\|_{L^{2}(0,T)} = \frac{\left|-(v,\partial_{t}\bar{u})_{L^{2}(\Sigma)}\right|}{\|\partial_{t}\bar{u}\|_{L^{2}(0,T)}} \leq \sup_{u \in H^{1}_{0,.}(0,T) \setminus \{0\}} \frac{\left|-(v,\partial_{t}u)_{L^{2}(\Sigma)}\right|}{\|\partial_{t}u\|_{L^{2}(0,T)}} = \|\omega\|_{[H^{1}_{0,.}(0,T)]'}.$$

Lemma A.1 implies the existence of the inverse of the (weak) time derivative, i.e., $\overline{\partial}_t^{-1}: [H_{0,}^1(0,T)]' \to L^2(0,T)$, which is also an isomorphism. As discussed earlier, we also have $\overline{\partial}_t^{-1}: L^2(\Sigma) \to H_{,0}^1(\Sigma)$. Hence, by interpolation, we conclude that $\overline{\partial}_t^{-1}: [H_{0,}^{1/2}(0,T)]' \to H_{,0}^{1/2}(\Sigma)$ is an isomorphism as well. Moreover, it is also an isometry between these spaces.

Another important ingredient in this Appendix is the modified Hilbert transform \mathcal{H}_T introduced in [38, Section 2.4]. We point out that it can be seen as a mapping $\mathcal{H}_T: H^1_{0,}(\Sigma) \to H^1_{0,0}(\Sigma)$ or as a mapping $\mathcal{H}_T: H^{1/2}_{0,1}(\Sigma) \to H^{1/2}_{0,0}(\Sigma)$, which satisfy

$$\|u\|_{H_{0,1}^{1/2}(\Sigma)} = \|\mathcal{H}_T u\|_{H_{0,0}^{1/2}(\Sigma)}, \quad \text{and} \quad \|u\|_{H_{0,1}^{1/2}(\Sigma)} = \|\mathcal{H}_T u\|_{H_{0,0}^{1/2}(\Sigma)}.$$
 (45)

Similarly, we have the inverse modified Hilbert transform that induces the mappings $\mathcal{H}_T^{-1}: H_{.0}^1(\Sigma) \to H_{0.}^1(\Sigma)$ and $\mathcal{H}_T^{-1}: H_{.0}^{1/2}(\Sigma) \to H_{0.}^{1/2}(\Sigma)$, which verify

$$\|u\|_{H_{0}^{1}(\Sigma)} = \|\mathcal{H}_{T}^{-1}u\|_{H_{0}^{1}(\Sigma)}, \quad \text{and} \quad \|u\|_{H_{0}^{1/2}(\Sigma)} = \|\mathcal{H}_{T}^{-1}u\|_{H_{0}^{1/2}(\Sigma)}.$$
 (46)

Now we are in the position to state the main result of this Appendix:

Proposition A.2. The following representation of the $[H_0^{1/2}(\Sigma)]'$ inner product holds:

$$(\omega, \eta)_{[H_0^{1/2}(\Sigma)]'} \equiv \left\langle \overline{\partial}_t^{-1} \omega, \overline{\partial}_t \mathcal{H}_T^{-1} \partial_t^{-1} \eta \right\rangle_{\Sigma}$$
 (47)

for $\omega, \eta \in [H_{0,}^{1/2}(\Sigma)]'$. Moreover, when $u, v \in L^2(\Sigma)$ (as piecewise linear functions do), we can further simplify this expression to

$$(u, v)_{[H_{0,}^{1/2}(\Sigma)]'} \equiv -\left\langle \mathcal{H}_T u, \overline{\partial}_t^{-1} v \right\rangle_{\Sigma}. \tag{48}$$

Next, we introduce some intermediate results in order to proceed to prove Proposition A.2. We begin by the following auxiliary lemma, which is closely related to [38, Lem. 2.3].

Lemma A.3. For $u \in H^{1/2}_{,0}(\Sigma)$ we have

$$\langle \partial_t \mathcal{H}_T^{-1} u, v \rangle_{\Sigma} = -\langle \mathcal{H}_T \partial_t u, v \rangle_{\Sigma}, \quad \text{for all } v \in H_0^{1/2}(\Sigma).$$

Proof. The proof works analogously to Lemma 2.3 in [38] but we include it for completeness. Consider a function $\varphi \in C^{\infty}(0,T)$ with $\varphi(T) = 0$. We remind the reader that it can be expanded as follows

$$\varphi(t) = \sum_{k=0}^{\infty} \varphi_k \cos\left[\left(\frac{\pi}{2} + k\pi\right) \frac{t}{T}\right],$$

where

$$\varphi_k := \frac{2}{T} \int_0^T \varphi(t) \cos \left[\left(\frac{\pi}{2} + k\pi \right) \frac{t}{T} \right] dt.$$

By definition of the inverse modified Hilbert transform \mathcal{H}_T^{-1} , we have that

$$\mathcal{H}_T^{-1}\varphi(t) = \sum_{k=0}^{\infty} \varphi_k \sin\left[\left(\frac{\pi}{2} + k\pi\right)\frac{t}{T}\right],$$

From the above expression it becomes clear that

$$\partial_t \mathcal{H}_T^{-1} \varphi(t) = \frac{1}{T} \sum_{k=0}^{\infty} \varphi_k \cos \left[\left(\frac{\pi}{2} + k\pi \right) \frac{t}{T} \right] \left(\frac{\pi}{2} + k\pi \right). \tag{49}$$

Additionally, we have that

$$\partial_t \varphi = -\frac{1}{T} \sum_{k=0}^{\infty} \varphi_k \sin\left[\left(\frac{\pi}{2} + k\pi\right) \frac{t}{T}\right] \left(\frac{\pi}{2} + k\pi\right). \tag{50}$$

Hence, by the definition of the modified Hilbert transform, we get

$$-\mathcal{H}_T \partial_t \varphi = \frac{1}{T} \sum_{k=0}^{\infty} u_k \cos \left[\left(\frac{\pi}{2} + k\pi \right) \frac{t}{T} \right] \left(\frac{\pi}{2} + k\pi \right) = \partial_t \mathcal{H}_T^{-1} \varphi, \tag{51}$$

for all $\varphi \in C^{\infty}(0,T)$ with $\varphi(T)=0$. Finally, the result follows by completion.

Similarly, we can prove

Lemma A.4. For $u \in H^1_0(\Sigma)$ we have

$$\langle \partial_t \mathcal{H}_T^{-1} u, v \rangle_{\Sigma} = -\langle \mathcal{H}_T \partial_t u, v \rangle_{\Sigma}, \quad \text{for all } v \in H^1_{.0}(\Sigma).$$

Finally, we conclude this Appendix by proving its main result.

Proof of Proposition A.2. We proceed by showing that: (i) the introduced bilinear forms can be used to represent the $[H_0^{1/2}(\Sigma)]'$ -norm (i.e., that they are continuous and elliptic); and (ii) they are symmetric. With these two pieces, and by using the polarization identity on Hilbert spaces, we conclude the desired inner-product representations.

 $\frac{Step\ 1:\ The\ bilinear\ form\ induces\ the\ [H_{0,}^{1/2}(\Sigma)]'\ norm.}{\text{First, we point out that, by composition,}\ \mathcal{H}_{T}^{-1}\overline{\partial}_{t}^{-1}:[H_{0,}^{1/2}(\Sigma)]'\to H_{0,}^{1/2}(\Sigma)\ \text{is an}}$ isometric isomorphism, hence

$$\left\| \mathcal{H}_{T}^{-1} \overline{\partial}_{t}^{-1} \omega \right\|_{H_{0}^{1/2}(\Sigma)} = \left\| \omega \right\|_{[H_{0,}^{1/2}(\Sigma)]'}. \tag{52}$$

Furthermore, by (40), we have that for $\omega \in [H_{0,}^{1/2}(\Sigma)]'$

$$\begin{split} \left\| \mathcal{H}_{T}^{-1} \overline{\partial}_{t}^{-1} \omega \right\|_{H_{0,}^{1/2}(\Sigma)}^{2} &= \left\langle \mathcal{H}_{T} \mathcal{H}_{T}^{-1} \overline{\partial}_{t}^{-1} \omega , \, \partial_{t} \mathcal{H}_{T}^{-1} \overline{\partial}_{t}^{-1} \omega \right\rangle_{\Sigma} \\ &= \left\langle \overline{\partial}_{t}^{-1} \omega , \, \partial_{t} \mathcal{H}_{T}^{-1} \overline{\partial}_{t}^{-1} \omega \right\rangle_{\Sigma}, \end{split}$$

which proves that the bilinear form on the right hand side of (47) does indeed represent the $[H_{0,}^{1/2}(\Sigma)]'$ -norm.

Finally, for $u \in L^2(\Sigma)$, we can use Lemma A.3 and get

$$\left\|\mathcal{H}_{T}^{-1}\overline{\partial}_{t}^{-1}u\right\|_{H_{0}^{1/2}(\Sigma)}^{2} = \left\langle\overline{\partial}_{t}^{-1}u,\,\partial_{t}\mathcal{H}_{T}^{-1}\overline{\partial}_{t}^{-1}u\right\rangle_{\Sigma} = -\left\langle\overline{\partial}_{t}^{-1}u,\,\mathcal{H}_{T}u\right\rangle_{\Sigma},$$

from where we conclude that the bilinear form on the right hand side of (48) induces the $[H_0^{1/2}(\Sigma)]'$ -norm.

Step 2: The obtained bilinear forms are symmetric.

From [38, Corollary 2.5], we know that

$$\langle \mathcal{H}_T w, \partial_t z \rangle_{\Sigma} = \langle \partial_t w, \mathcal{H}_T z \rangle_{\Sigma}, \quad \forall w, z \in H_{0,}^{1/2}(\Sigma).$$

Hence

$$\begin{split} \left\langle \overline{\partial}_{t}^{-1}\omega\,,\,\partial_{t}\mathcal{H}_{T}^{-1}\overline{\partial}_{t}^{-1}\eta\right\rangle _{\Sigma} &= \left\langle \mathcal{H}_{T}(\mathcal{H}_{T}^{-1}\overline{\partial}_{t}^{-1}\omega)\,,\,\partial_{t}(\mathcal{H}_{T}^{-1}\overline{\partial}_{t}^{-1}\eta)\right\rangle _{\Sigma} \\ &= \left\langle \partial_{t}(\mathcal{H}_{T}^{-1}\overline{\partial}_{t}^{-1}\omega)\,,\,\mathcal{H}_{T}(\mathcal{H}_{T}^{-1}\overline{\partial}_{t}^{-1}\eta)\right\rangle _{\Sigma} \\ &= \left\langle \partial_{t}\mathcal{H}_{T}^{-1}\overline{\partial}_{t}^{-1}\omega\,,\,\overline{\partial}_{t}^{-1}\eta\right\rangle _{\Sigma}, \end{split}$$

for
$$\omega, \eta \in [H_{0,}^{1/2}(\Sigma)]'$$
, and

$$-\left\langle \overline{\partial}_t^{-1} u, \mathcal{H}_T v \right\rangle_{\Sigma} = -\left\langle \mathcal{H}_T u, \overline{\partial}_t^{-1} v \right\rangle_{\Sigma}, \quad \forall u, v \in L^2(\Sigma).$$